

Supplementary information of

Large magnetic anisotropy and rotating cryomagnetocaloric effect in single-crystalline paramagnetic lanthanide calcium oxyborates $\text{LnCa}_4\text{O}(\text{BO}_3)_3$ with $\text{Ln} = \text{Pr}, \text{Nd}, \text{Gd}, \text{Er}, \text{Tm}$

Fatiha Azrour ^a, Romain Viennois ^{a,*}, Jérôme Long ^{a,b}, Corine Reibel ^a, Jérôme Debray ^c, Fapeng Yu ^d,
Shujun Zhang ^e, Mickaël Beaudhuin ^{a,#}, Jérôme Rouquette ^{a,#}

^a ICGM, Univ Montpellier, CNRS, ENSCM, Montpellier, France

^b Institut Universitaire de France (IUF), 1 rue Descartes, 75231 Paris Cedex 05, France

^c Institut Néel, CNRS and Université Grenoble Alpes, BP166, F-38042 Grenoble Cedex 9, France

^d State Key Laboratory of Crystal Materials, Shandong University, Jinan, China

^e Institute for Superconducting and Electronic Materials, Faculty of Engineering and Information
Science, University of Wollongong, North Wollongong, Australia

* Corresponding author email: romain.viennois@umontpellier.fr

#Emails: mickael.beaudhuin@umontpellier.fr, jerome.rouquette@umontpellier.fr

Crystallographic data of single-crystalline $\text{LnCa}_4\text{O}(\text{BO}_3)_3$ samples

The details of the crystal structure can be found in the cif files available at CCDC.

We report the interatomic distances (in Angstroms) around the lanthanide and Ca ions in the different Ln, M1 and M2 sites for the different samples of $\text{LnCa}_4\text{O}(\text{BO}_3)_3$ at 100 K in the Table S1-S5 which were obtained from analysis of XRD data.

Table S1: Interatomic distances (in Å) Ln-O, M1-O and M2-O in single-crystalline $\text{PrCa}_4\text{O}(\text{BO}_3)_3$ at 100 K.

PrCOB	O₄	O₄	O₆	O₆	O₃	O₃
Ln	2.475(4)	2.475 (4)	2.403(4)	2.490(3)	2.296(3)	2.270(3)
	O₃	O₅	O₁	O₁	O₂	O₂
M1	2.316(2)	2.335(3)	2.363(2)	2.372(3)	2.334(1)	2.401(2)
	O₁	O₂	O₄	O₄	O₅	O₅
M2	2.336(3)	2.512(2)	2.342(2)	2.329(2)	2.459(3)	2.588(3)

Table S2: Interatomic distances (in Å) Ln-O, M1-O and M2-O in single-crystalline $\text{NdCa}_4\text{O}(\text{BO}_3)_3$ at 100 K.

NdCOB	O₄	O₄	O₆	O₆	O₃	O₃
Ln	2.455(3)	2.455(3)	2.387(5)	2.479(4)	2.290(5)	2.267(6)
	O₃	O₅	O₁	O₁	O₂	O₂
M1	2.317(3)	2.338(3)	2.361(3)	2.371(3)	2.333(3)	2.393(3)
	O₁	O₂	O₄	O₄	O₅	O₅
M2	2.333 (3)	2.505(3)	2.343(3)	2.337(3)	2.455(3)	2.596(3)

Table S3: Interatomic distances (in Å) Ln-O, M1-O and M2-O in single-crystalline GdCa₄O(BO₃)₃ at 100 K.

GdCOB	O₄	O₄	O₆	O₆	O₃	O₃
Ln	2.393(3)	2.393(3)	2.339(6)	2.426(5)	2.248(5)	2.246(6)
	O₃	O₅	O₁	O₁	O₂	O₂
M1	2.329(4)	2.340(3)	2.353(3)	2.361(4)	2.315(3)	2.373(3)
	O₁	O₂	O₄	O₄	O₅	O₅
M2	2.336(3)	2.466(3)	2.345(3)	2.334(3)	2.460(4)	2.618(3)

Table S4: Interatomic distances (in Å) Ln-O, M1-O and M2-O in single-crystalline ErCa₄O(BO₃)₃ at 100 K.

ErCOB	O₄	O₄	O₆	O₆	O₃	O₃
Ln	2.349(2)	2.349(2)	2.316(4)	2.381(3)	2.249(3)	2.222(4)
	O₃	O₅	O₁	O₁	O₂	O₂
M1	2.324(2)	2.342(2)	2.354(2)	2.358(2)	2.346(2)	2.296(2)
	O₁	O₂	O₄	O₄	O₅	O₅
M2	2.336(2)	2.443(2)	2.335(1)	2.343(2)	2.465(2)	2.627(2)

Table S5: Interatomic distances (in Å) Ln-O, M1-O and M2-O in single-crystalline TmCa₄O(BO₃)₃ at 100 K.

TmCOB	O₄	O₄	O₆	O₆	O₃	O₃
Ln	2.345(4)	2.345(4)	2.310(7)	2.374(6)	2.245(5)	2.223(6)
	O₃	O₅	O₁	O₁	O₂	O₂
M1	2.319(4)	2.341(4)	2.353(3)	2.359(4)	2.340(4)	2.291(3)
	O₁	O₂	O₄	O₄	O₅	O₅
M2	2.332(4)	2.439(4)	2.331(3)	2.340(4)	2.465(4)	2.624(3)

Table S6: Distortion index for the bond lengths $d(\text{length})$ and the bond angle variance $\sigma(\text{angle})$ in deg.² of the different polyhedra around Ln, M1 and M2 sites for the single-crystalline LnCOB compounds at 100 K. Note that the polyhedra around M2 is not an octahedral in the case of Tm but one polyhedral with 7 atoms.

LnCOB	Ln		M1		M2	
	$d(\text{length})$	$\sigma(\text{angle})$	$d(\text{length})$	$\sigma(\text{angle})$	$d(\text{length})$	$\sigma(\text{angle})$
Pr	0.0329	139.52	0.0106	58.86	0.0378	276.59
Nd	0.0309	138.35	0.0098	60.22	0.0373	276.91
Gd	0.0259	128.19	0.0074	61.58	0.0361	278.51
Er	0.0215	114	0.0078	64.3	0.0357	282.2
Tm	0.021	111.11	0.0083	65.7	0.0569	

Additional data on the magnetic properties of powdered $\text{LnCa}_4\text{O}(\text{BO}_3)_3$ samples under ZFC

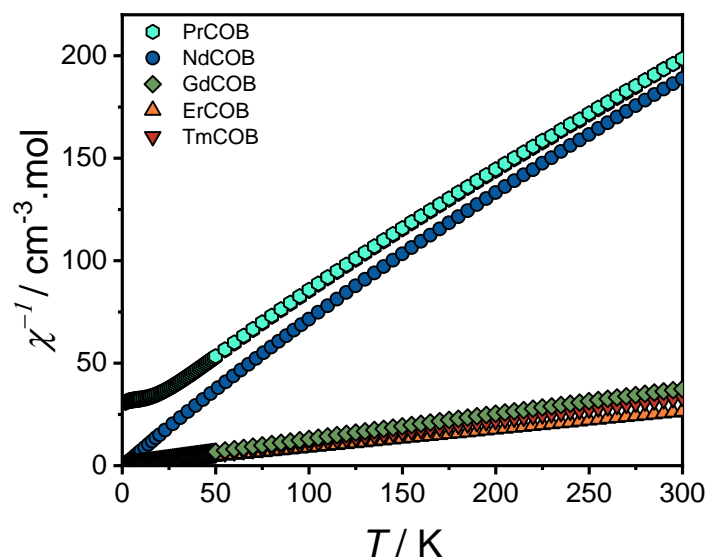


Figure S1: Temperature variation of the inverse of magnetic susceptibility of powdered $\text{LnCa}_4\text{O}(\text{BO}_3)_3$ ($\text{Ln} = \text{Pr, Nd, Gd, Er, Tm}$) samples.

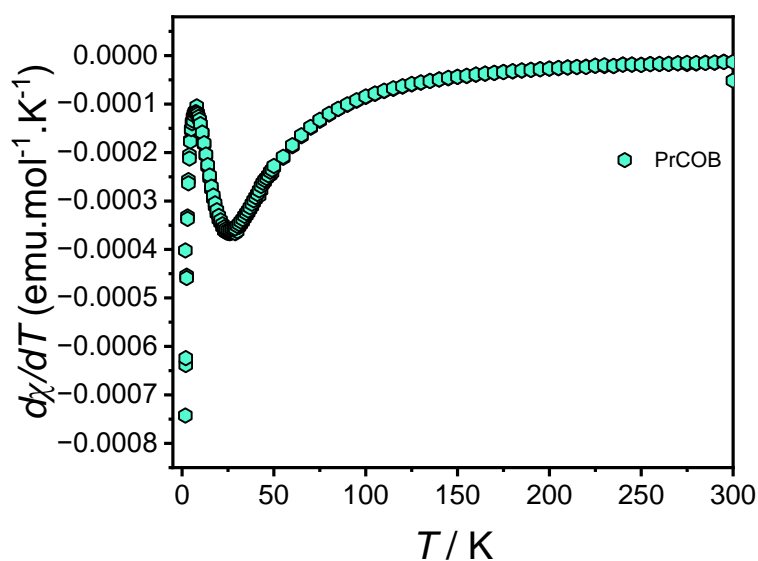


Figure S2: Temperature variation of the derivative of magnetic susceptibility of powdered $\text{PrCa}_4\text{O}(\text{BO}_3)_3$ sample.

Orientation of the single-crystalline samples

We have performed the study of the magnetic properties of single-crystalline $\text{LnOCa}_4(\text{BO}_3)_3$ ($\text{Ln} = \text{Pr}, \text{Nd}, \text{Gd}, \text{Er}, \text{Tm}$) for the different crystalline directions. For doing that, we have used samples cutted in the X-Y plan for $\text{Ln} = \text{Pr}, \text{Gd}, \text{Er}, \text{Tm}$ and we have studied the magnetic susceptibility as function of the orientation of the magnetic field in the X-Y and X-Z plans. The accuracy of the orientation with goniometer was about 10° and this is why it is difficult to obtain exactly the monoclinic angle of about 100° when doing the rotation in the X-Z plan. For $\text{Ln} = \text{Nd}$, the single-crystalline sample is oriented in the Y-Z plan and we have studied its magnetic susceptibility as function of the orientation of the magnetic field in the X-Z and Y-Z plans. The results at 300 K are given in the Figure S3 of the supplementary information for $\text{Ln} = \text{Pr}, \text{Nd}, \text{Er}, \text{Tm}$.

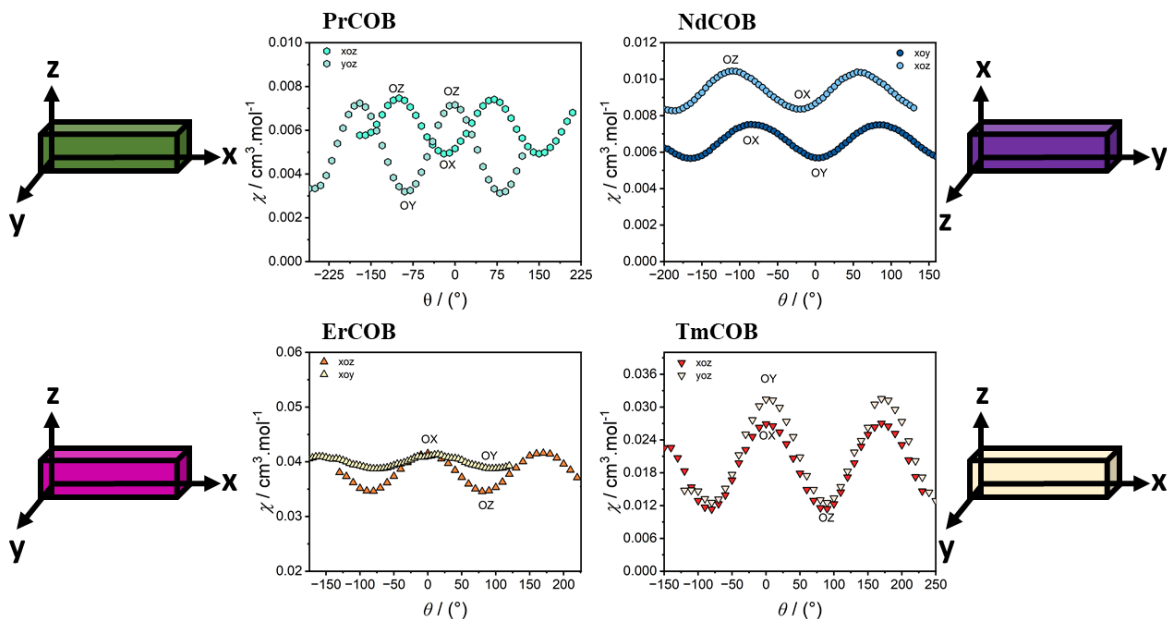


Figure S3: Orientation of single-crystalline $\text{LnCa}_4\text{O}(\text{BO}_3)_3$ ($\text{Ln} = \text{Pr}, \text{Nd}, \text{Er}, \text{Tm}$) samples and their magnetic susceptibility as function of the magnetic field orientation at 300 K.

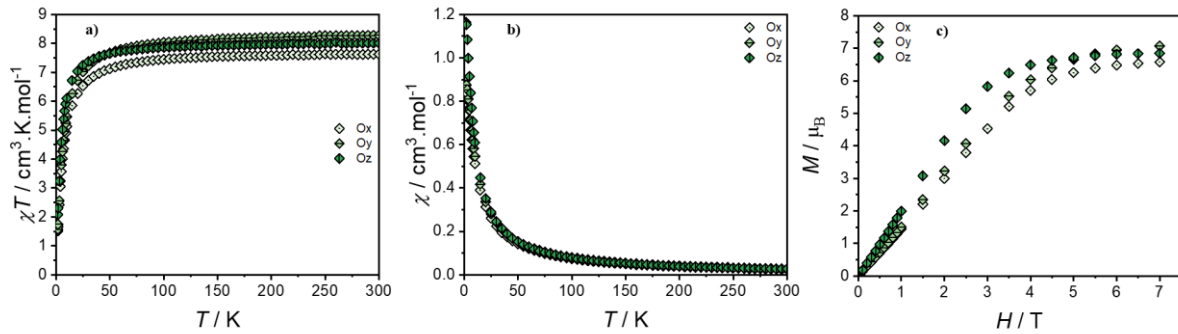


Figure S4: a) ZFC χT of single-crystalline $\text{GdCa}_4\text{O}(\text{BO}_3)_3$ as function of the temperature; b) ZFC magnetic susceptibility χ of single-crystalline $\text{GdCa}_4\text{O}(\text{BO}_3)_3$ as function of the temperature; c) isothermal magnetization M of single-crystalline $\text{GdCa}_4\text{O}(\text{BO}_3)_3$ at 1.8 K as function of the magnetic field.

Additional data on the magnetic properties of single-crystalline $\text{LnOCa}_4(\text{BO}_3)_3$ samples

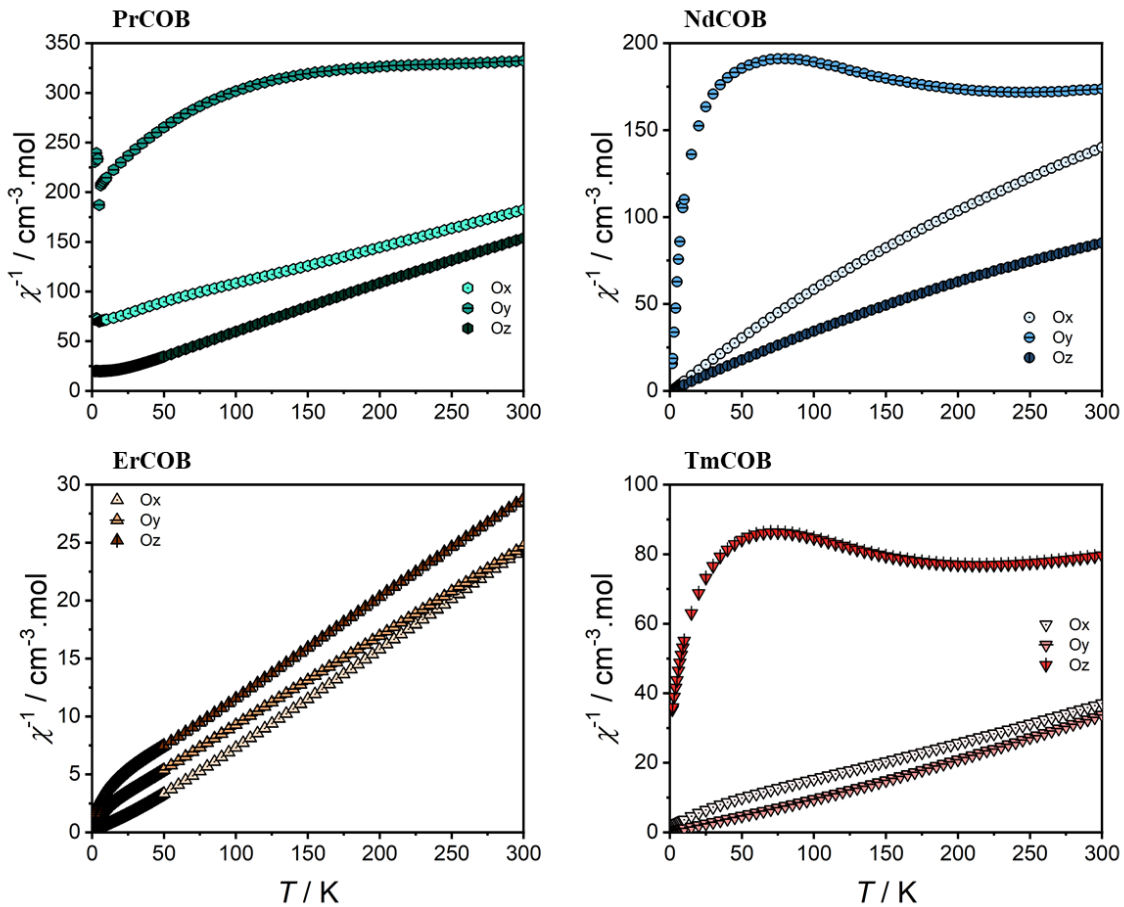


Figure S5: Temperature variation of the inverse of magnetic susceptibility of single-crystalline $\text{LnCa}_4\text{O}(\text{BO}_3)_3$ ($\text{Ln} = \text{Pr}, \text{Nd}, \text{Er}, \text{Tm}$) samples along the Ox, Oy and Oz directions under ZFC conditions.

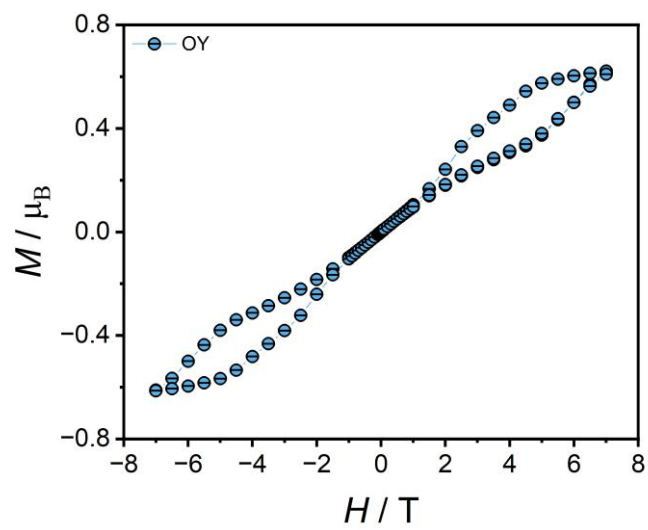


Figure S6: Hysteresis of single-crystalline NdCa₄O(BO₃)₃ sample along the Oy direction at 1.8 K.

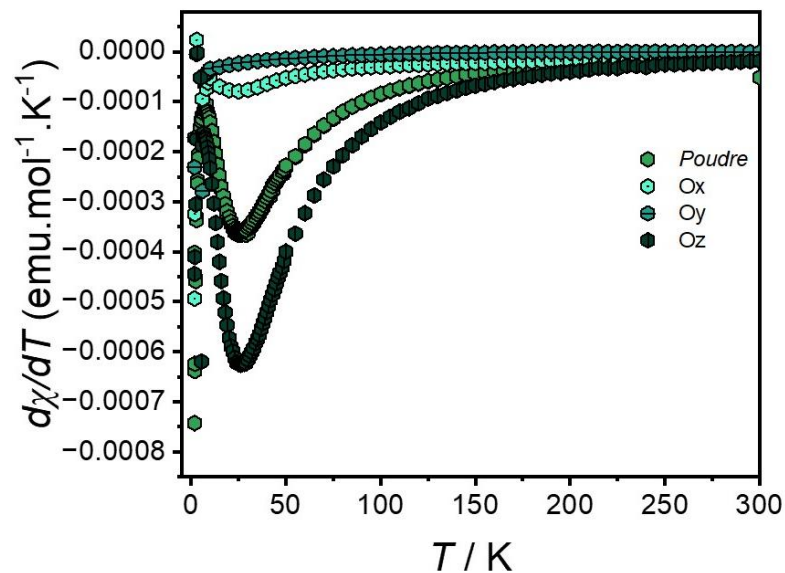


Figure S7: Temperature variation of the derivative of magnetic susceptibility of powdered and single-crystalline PrCa₄O(BO₃)₃ sample under ZFC conditions.

Table S7: χT at 300 K, effective moment μ_{eff} obtained from the Curie-Weiss law and magnetization at 7 T of single-crystalline $\text{LnOCa}_4(\text{BO}_3)_3$ samples with $\text{Ln} = \text{Nd}$ and Er .

NdCOB	$\chi^*T(300K)$	$\mu_{\text{eff}} (\mu_B)$	$M_{\text{sat}} (\mu_B / f.u)$	ErCOB	$\chi^*T(300K)$	$\mu_{\text{eff}} (\mu_B)$	$M_{\text{sat}} (\mu_B / f.u)$
Ox	2.26	3.74(0.022)	2.26	Ox	11.90	9.83(0.054)	7.34
Oy	1.75	-	0.67	Oy	11.82	10.01(0.054)	4.19
Oz	3.55	4.89(0.025)	2.77	Oz	9.98	9.35(0.042)	7.31

Table S8: χT at 300 K, effective moment μ_{eff} obtained from the Curie-Weiss law and magnetization at 7 T of single-crystalline $\text{LnOCa}_4(\text{BO}_3)_3$ samples with $\text{Ln} = Tm$ and Gd .

TmCOB	$\chi^*T(300K)$	$\mu_{\text{eff}} (\mu_B)$	$M_{\text{sat}} (\mu_B / f.u)$	GdCOB	$\chi^*T(300K)$	$\mu_{\text{eff}} (\mu_B)$	$M_{\text{sat}} (\mu_B / f.u)$
Ox	8.09	5.77(0.033)	2.47	Ox	7.63	7.93(0.04)	6.54
Oy	8.89	3.70(0.021)	5.67	Oy	8.28	8.24(0.045)	7.04
Oz	3.77	-	2.32	Oz	8.01	8.07(0.042)	6.85

Table S9: χT at 300 K, effective moment μ_{eff} obtained from the Curie-Weiss law and magnetization at 7 T of single-crystalline $\text{PrOCa}_4(\text{BO}_3)_3$ sample.

PrCOB	$\chi^*T(300K)$	$\mu_{\text{eff}} (\mu_B)$
Ox	1.644	4.603(0.008)
Oy	0.902	10.328(0.306)
Oz	1.950	4.172(0.025)

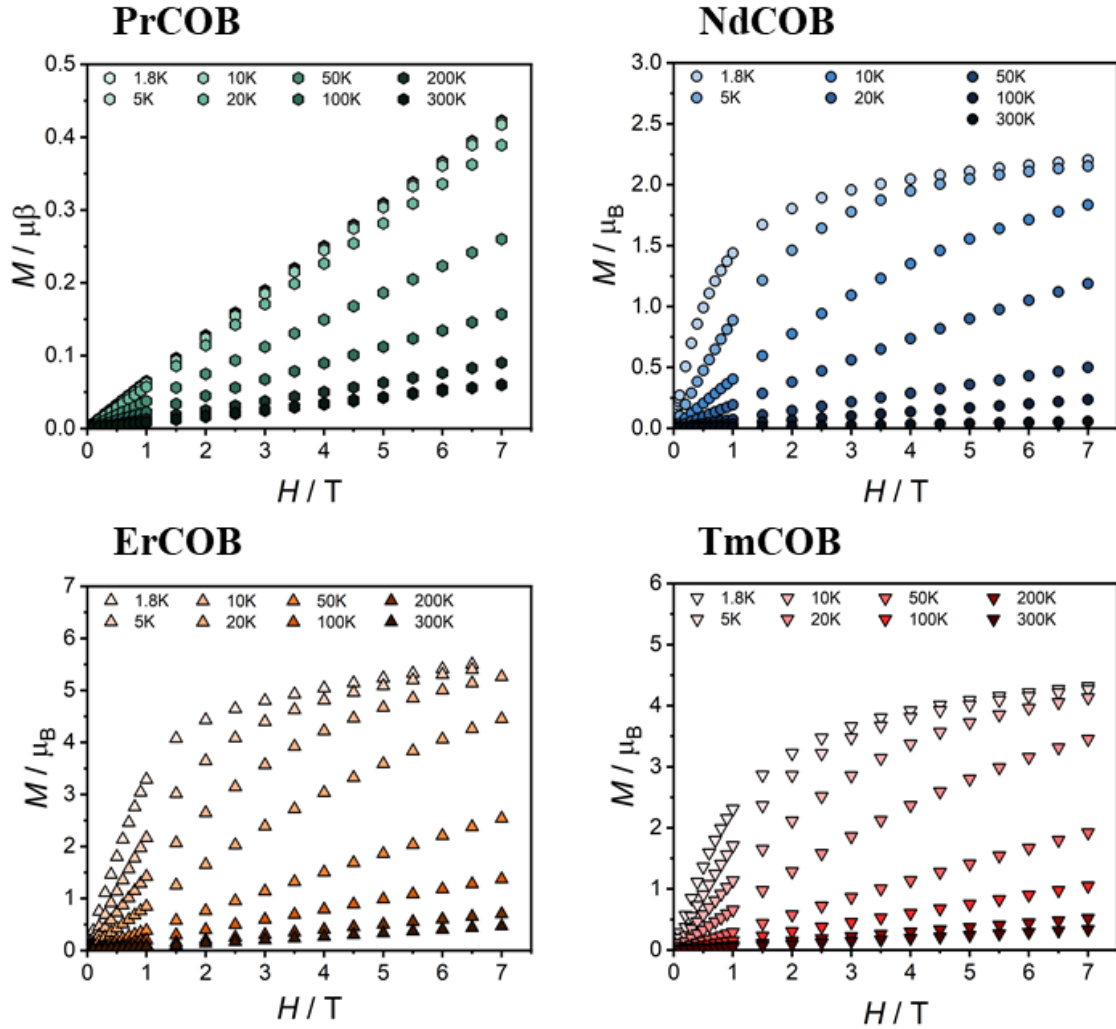


Figure S8: Isothermal magnetization M of powdered $\text{LnCa}_4\text{O}(\text{BO}_3)_3$ ($\text{Ln} = \text{Nd}, \text{Pr}, \text{Er}, \text{Tm}$) samples as function of the magnetic field. at different temperatures.

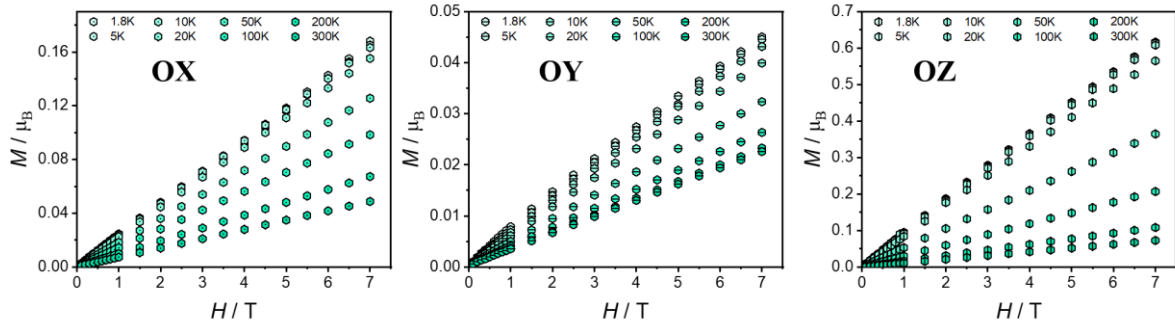


Figure S9: Isothermal magnetization M of single-crystalline $\text{PrCa}_4\text{O}(\text{BO}_3)_3$ sample along the different Ox , Oy and Oz directions as function of the magnetic field. at different temperatures.

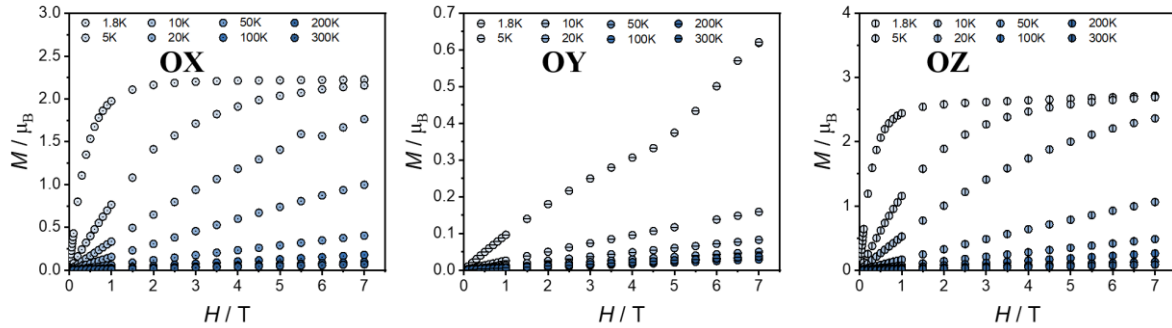


Figure S10: Isothermal magnetization M of single-crystalline $\text{NdCa}_4\text{O}(\text{BO}_3)_3$ sample along the different Ox, Oy and Oz directions as function of the magnetic field. at different temperatures.

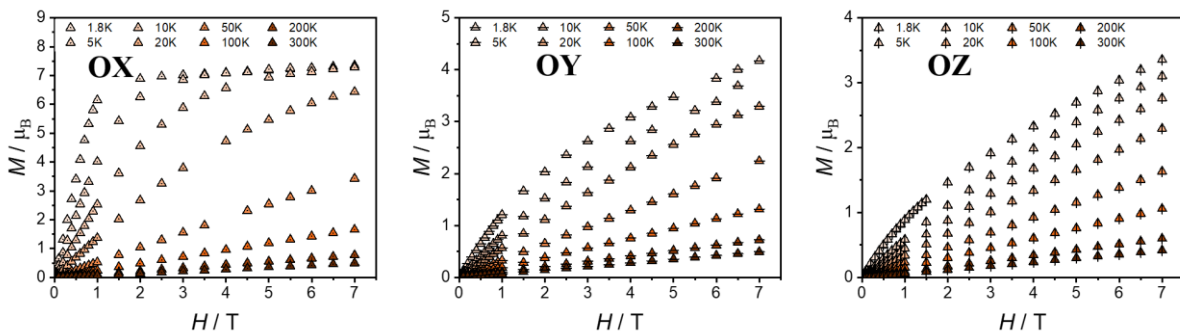


Figure S11: Isothermal magnetization M of single-crystalline $\text{ErCa}_4\text{O}(\text{BO}_3)_3$ sample along the different Ox, Oy and Oz directions as function of the magnetic field. at different temperatures.

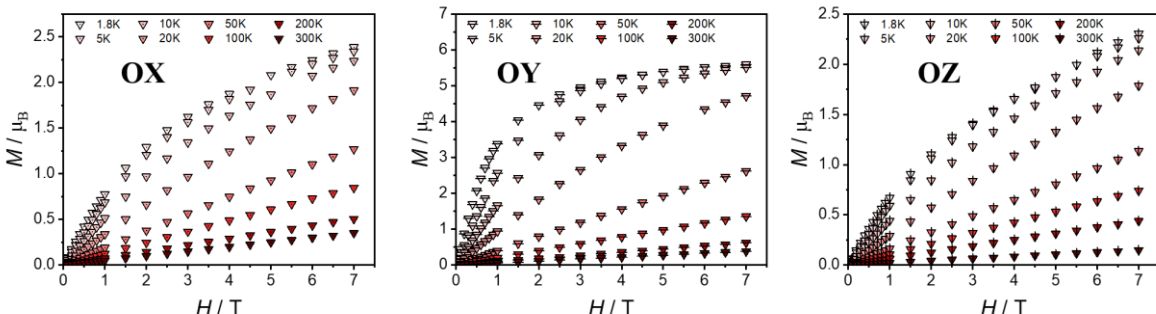


Figure S12: Isothermal magnetization M of single-crystalline $\text{TmCa}_4\text{O}(\text{BO}_3)_3$ sample along the different Ox, Oy and Oz directions as function of the magnetic field. at different temperatures.